Analysis and Optimization of the HARQ-Based Spinal Coded Timely Status Update System

Siqi Meng, Shaohua Wu, *Member, IEEE*, Aimin Li, *Student Member, IEEE*, Jian Jiao, *Member, IEEE*, Ning Zhang, *Senior Member, IEEE*, and Qinyu Zhang, *Senior Member, IEEE*

***Abstract*— The age of information (AoI) is a new metric to measure the timeliness of various status update systems, and hybrid automatic repeat request (HARQ) transmission scheme is usually applied to ensure higher timeliness. However, little research considers encoding delay, propagation delay, decoding delay and feedback delay in the HARQ-based coded status update system. To the best of our knowledge, in this paper, the HARQ-based Spinal coded timely status update system with all the practical delay elements is considered for the first time. We derive the average AoI expression of the system and analyze the monotony of the AoI expression to give an average AoI upper bound. Then we optimize the HARQ transmission scheme to minimize the AoI. To decrease the complexity of the optimization algorithm, we separate it into two steps. First, we optimize the puncturing pattern of Spinal codes and propose a transmission scheme under incremental tail transmission puncturing (ITTP) pattern. Second, we optimize the number of symbols in each round under the ITTP transmission scheme, and propose the optimal transmission scheme under the coarse-grained ITTP pattern. Simulation results show that the proposed transmission scheme can significantly decrease the AoI compared to the baseline transmission schemes.**

***Index Terms*— Age of information (AoI), Spinal codes, hybrid automatic repeat request (HARQ), timely status update system, transmission scheme.**

I. Introduction

DRIVEN by the increasing research attention of the timeliness of information in the status update systems such as vehicular networks [1] and remote control systems [2], the age of information (AoI) is a new metric to measure the freshness of the update information [3]. AoI measures the time that has elapsed since the status update was generated. Specifically, if a status update is generated at the timestamp $U(t)$, then at time t the age of the update is $\Delta = t - U(t)$. The AoI of the status update system will continuously increase until an update is successfully received, with the AoI updated to Δ. In the literature, there are many previous works on the AoI from various perspectives, including multiple-server queuing system [4], [5], wireless network system optimization [6], [7], reinforcement learning [8] and game theory [9]. Note that in these researches the status updates are assumed to be always successfully received.

Nevertheless, for the practical transmission process in the physical layer, the status updates will be disturbed by noises in the unreliable channels, so the status updates are not always successfully received. In this case, channel coding is applied to decrease the error probability of status updates. For the coded status update system, the AoI depends on the probability of failed transmission. Specifically, lower error probability of the coded status updates will result in lower AoI of the system. To further ensure high timeliness of the system, transmission schemes such as automatic repeat request (ARQ) and hybrid ARQ (HARQ) are usually applied in the coded status update system to enhance reliable transmission.

In [10], the optimal scheduling policies for ARQ and HARQ transmission scheme under the resource constraint with unknown error probability are studied to decrease the AoI of the noisy channel systems. In [11], the average AoI expressions of fixed-rate code and rateless code over binary erasure channel with non-ARQ transmission scheme are theoretically analyzed. The status update queuing system over erasure channels is studied in [12], where the AoI expressions of the ARQ- and HARQ-based coded system under finite code length are derived by using the finite-block-length information theory bound of the block error rate. As for the transmission scheme design of the HARQ-based coded status update system, the authors find out that the optimal code lengths form a threshold structure, where a new update is transmitted only if the AoI of the system reaches a threshold [13]. Moreover, under HARQ transmission scheme, the average AoI expression with regard to the code length and the error probability is analytically derived in [14].

Some researches also consider the AoI of specific channel codes. In [15], the authors theoretically analyze the average AoI expressions of low-density parity-check (LDPC) coded status update system with ARQ, truncated ARQ and HARQ transmission schemes. In the recent work of [16], the timeliness of Polar coded status update system is studied, and

Manuscript received 24 January 2022; revised 8 June 2022; accepted 5 August 2022. Date of publication 11 August 2022; date of current version 18 October 2022. This work has been supported in part by the National Natural Science Foundation of China under Grant nos. 61871147, 62071141, and in part by the Shenzhen Science and Technology Program under Grant nos. GXWD20201230155427003-20200730122528002, ZDSYS20210623091808025, and in part by the Major Key Project of PCL under Grant no. PCL2021A03-1. The associate editor coordinating the review of this article and approving it for publication was H. Zhang. *(Corresponding author: Shaohua Wu.)*

Siqi Meng and Aimin Li are with the Department of Electronic and Information Engineering, Harbin Institute of Technology, Shenzhen 518055, China (e-mail: mengsiqi@stu.hit.edu.cn; liaimin@stu.hit.edu.cn).

Shaohua Wu, Jian Jiao, and Qinyu Zhang are with the Department of Electronic and Information Engineering, Harbin Institute of Technology, Shenzhen 518055, China, and also with the Peng Cheng Laboratory, Shenzhen 518055, China (e-mail: hitwush@hit.edu.cn; jiaojian@hit.edu.cn; zqy@hit.edu.cn).

Ning Zhang is with the Department of Electrical and Computer Engineering, University of Windsor, Windsor, ON N9B 3P4, Canada (e-mail: ning.zhang@uwindsor.ca).

Color versions of one or more figures in this article are available at https://doi.org/10.1109/TCOMM.2022.3198122.

Digital Object Identifier 10.1109/TCOMM.2022.3198122

the average AoI expressions of the systems with different transmission schemes, including classic ARQ, HARQ with chase combining (HARQ-CC) and HARQ with incremental redundancy (HARQ-IR), are derived respectively. But these previous works only consider the transmission delay of the system, which restricts their applications in practical status update systems. However, the delays from the encoding, propagation, decoding and feedback process will also increase the AoI of the system, which cannot be neglected in practice. As such, the timeliness of the HARQ-based coded status update system considering all the practical delay elements is still to be studied.

Spinal codes are new rateless codes first proposed in [17], which have been proved to achieve the Shannon capacity over both the additive white Gaussian noise (AWGN) channel and the binary symmetric channel (BSC) [18]. Because of the high rate of Spinal codes over the AWGN channel, fewer code symbols are needed to be sent in the transmission process of a Spinal coded status update frame, which results in lower transmission delay and lower AoI. Furthermore, Spinal codes can achieve seamless rate adaptation by simple transmission scheme with puncturing, which is an advantage over fixed-rate coding scheme such as LDPC codes and Polar codes. Analyzing and optimizing the AoI performance of Spinal coded timely status update system is of great importance in the practical applications, for the lower AoI of Spinal coded system will fundamentally achieve higher timeliness of the whole status update system.

Researchers have worked on improving Spinal coding schemes since Spinal codes were proposed, such as compressing the sparse source at the sender side to increase the throughput [19], applying unequal error protection structure to achieve lower error probability [20], [21], introducing novel and dynamic decoding algorithm at the receiver side to decrease the decoding complexity [22], and proposing new Spinal coding structure to improve the performance [23], [24]. However, few works have studied the optimization of the transmission scheme of Spinal codes in the HARQ-based status update system from the AoI perspective.

In this paper, we study the timeliness of the HARQ-based Spinal coded timely status update system for the first time. We introduce a more practical system model with encoding delay, transmission delay, propagation delay, decoding delay and feedback delay. We derive the expressions of these types of delays in the Spinal coded status update system according to the coding structure and transmission scheme of Spinal codes, and give the AoI evolution process of status update system considering these types of delays.

Then, we derive the average AoI expression of the HARQ-based Spinal coded system associated with these types of delays and the probability of successful decoding. By numerically analyzing the monotony of the AoI expression with the probability of successful decoding, we find out that when the decoding delay is close to or much larger than transmission delay, the derivative of AoI expression with regard to the probability of successful decoding is always negative. This implies that the average AoI of the system can be upper bounded by the lower bound of the probability of successful decoding (or the upper bound of failed decoding) for the HARQ-based Spinal coded system when the decoding delay is rather large. Based on the frame error rate (FER) upper bound of Spinal codes in each HARQ transmission round, we give the average AoI upper bound of the HARQ-based Spinal coded status update system, which we will use as the objective function in the following optimization problem.

Furthermore, we optimize the transmission scheme of the HARQ-based Spinal coded system to achieve minimum AoI, under the constraint of the number of total code symbols. Minimizing the AoI of a system does not necessarily mean minimizing a certain type of delay. For example, if very few code symbols are transmitted at the first few rounds, then the transmission delay in each round is minimized. However, such few received code symbols may cause a high probability of decoding failure, which results in more incremental transmission rounds and larger decoding delay. In this case, the minimization of the transmission delay may contrarily increase the AoI.

In the optimization problem, the HARQ transmission scheme is optimized by two steps. The reason for separating the optimization algorithm into two steps is that the HARQ transmission scheme consists of two degree of freedom, namely the number of symbols transmitted in each round and the puncturing pattern of Spinal codes in each round. Directly optimizing the transmission scheme will result in extremely high computing complexity. Therefore, we propose a two-step optimization method, by which the following optimization problems can be simplified. First we optimize the puncturing pattern in each round by restricting the number of symbols as one. Solving this problem, we can find out the best puncturing positions for each code symbols. Using this best puncturing pattern, we next optimize the allocation of the number of code symbols in each round to find out the whole transmission scheme with minimum AoI.

Specifically, the first step is to find out the best puncturing positions in each round, where we consider and optimize the symbol-by-symbol transmission scheme (called the transmission scheme under the most fine-grained puncturing pattern). Solving the optimization problem by iterative algorithm, we propose a transmission scheme under the most fine-grained incremental tail transmission puncturing (ITTP) pattern to improve the AoI performance compared to the transmission scheme under uniform puncturing (UP) pattern. The second step is to find out the best allocation of the number of code symbols in each round, where we consider a more general transmission scheme where more than one symbols are transmitted in the incremental rounds (called the transmission scheme under coarse-grained puncturing pattern), and we use an exhaustive searching algorithm to solve this optimization problem. Combining the two solutions of the two optimization problems, we finally propose the optimal transmission scheme under coarse-grained ITTP pattern at different signal-to-noise ratio (SNR), as a refinement of the most fine-grained ITTP pattern. Simulation results demonstrate that the proposed optimal transmission scheme can further improve

higher timeliness compared to the baseline transmission schemes.

The main contributions of this paper are summarized as follows:

- To the best of our knowledge, this is the first study to analyze the HARQ-based coded timely status update systems with various types of delays, including encoding delay, transmission delay, propagation delay, decoding delay and feedback delay. Considering these delays, we study the AoI evolution process of the HARQ-based Spinal coded status update system.
- We derive the average AoI expression of Spinal coded status update system, and analyze the monotony of the average AoI. Based on the monotony analysis of the average AoI with the probability of successful decoding in each round, we further give an average AoI upper bound of the Spinal coded status update system.
- Leveraging the average AoI upper bound as the objective function, we optimize the HARQ transmission scheme of Spinal coded status update system by solving a two-step optimization problem, and propose the optimal transmission scheme under the coarse-grained ITTP pattern.

The rest of the paper is organized as follows: Section II gives the basis of Spinal codes, including the encoding process, decoding algorithms, puncturing patterns and transmission schemes. Section III introduces the system model of the HARQ-based Spinal coded status update system, and analyzes the different types of delays and AoI evolution of the system. In Section IV, the average AoI expression and upper bound of the HARQ-based Spinal coded system are theoretically analyzed. Section V focuses on the optimization of the transmission scheme for the HARQ-based Spinal coded system to minimize the AoI. Numerical results are given in Section VI and Section VII concludes the paper.

II. Preliminaries

A. Encoding Process of Spinal Codes

Spinal codes employ hash function and the random numeral generator (RNG) to encode the source message as pseudo random code symbols. As depicted in Fig. 1, the encoding process of Spinal codes contains four main steps.

Step 1: Dividing message into blocks. An n-bit source message M is divided into n/k message blocks called m_i, $i = 1, 2, \ldots n/k$, with each block containing k bits. After dividing, the source message is $M = [m_1, m_2, \ldots, m_{n/k}]$.

Step 2: Hash mapping to generate spine value s. The hash function h maps the two inputs, which are a k-bit message m_i and a v-bit spine value s_{i-1}, to an output v-bit spine value s_i, that is $s_i = h(s_{i-1}, m_i), i = 1, 2, \ldots n/k$. Usually we choose the initial spine value as $s_0 = 0$ to initialize the mapping, which is known by both the encoder and the decoder.

Step 3: RNG mapping to generate code symbols. The spine value s_i serves as the seed of RNG, and the RNG of the message block m_i will generate c-bit code symbols called $x_{i,j}$, where j represents the pass of the corresponding symbols.

Step 4: Channel constellation mapping (modulation). The output code symbols from the encoder will be modulated

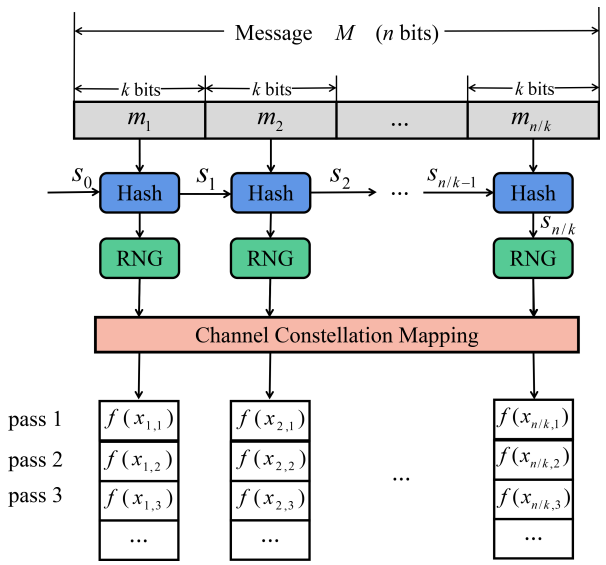

Fig. 1. The encoding structure of Spinal codes.

to adjust to the channel condition. In this paper, we use the uniform constellation mapping [17], where the c-bit code symbol $x_{i,j}$ is mapped as a number $f(x_{i,j}) = \frac{u-1/2}{\sqrt{6P}}$, where $u = \frac{x_{i,j}+1/2}{2^c}$ and $P = \frac{(2^c+1)(2^c-1)}{12}$.

B. Decoding Algorithm of Spinal Codes

The maximum likelihood (ML) decoding is the optimal decoding algorithm for Spinal codes, where the decoder searches for the candidate message whose encoded symbols are the closest with the received symbols. The ML rule of Spinal codes is mathematically expressed as follows:

$$\hat{M} \in \arg\min ||y - f(x(M'))||^2, M' \in \{0,1\}^n, \quad (1)$$

where $\hat{M}$ denotes the output of the decoder, y the received symbols and $f(x(M'))$ the encoded symbols corresponding to the candidate message M'.

However, the complexity of ML decoding algorithm is exponential with the message length, which makes it impractical in hardware implementation for long messages. Spinal codes are tree codes with serial coding structure, so the tree pruning algorithm, also called bubble decoding algorithm, can be used for Spinal codes. In the bubble decoding algorithm with pruning depth B, only B nodes whose path costs are the least will remain in each layer, by which the complexity is reduced to the polynomial level. In this paper, bubble decoding is applied as a default.

C. Puncturing Patterns and Transmission Schemes of Spinal Codes

The transmission scheme for Spinal codes includes the puncturing patterns in each transmission round and the number of code symbols transmitted in each round. We denote $\mathcal{N} = [(\nu_1, \mathbf{L}_1), (\nu_2, \mathbf{L}_2), \ldots, (\nu_r, \mathbf{L}_r)]$ as the total transmission scheme, where ν_i represents the number of symbols that have been transmitted from round 1 to round i, and $\mathbf{L}_i = [l_{i,1}, l_{i,2}, \ldots, l_{i,n/k}]$ represents the puncturing pattern

at round i, where $l_{i,j}$ is the number of symbols corresponding to jth spine value.

In the normal transmission scheme for Spinal codes, the code symbols are transmitted pass by pass, as shown in Fig. 1. Specifically, firstly several passes (or one pass) of symbols are transmitted, and if the decoding fails, the sender will continuously transmit incremental passes of symbols until a successful decoding. In such transmission scheme, the number of code symbols incrementally transmitted in each round is equal to the number of message blocks, and we have $l_{i,1} = l_{i,2} = \ldots = l_{i,n/k}$ for each $\mathbf{L}_i$.

To further improve the rate performance of Spinal codes, the transmission scheme with puncturing is proposed in [17]. In the transmission scheme with puncturing, the whole pass is divided into n/k sub-passes, and instead of sending the whole pass, only a certain sub-pass will be transmitted after a decoding failure. Fig. 2 shows a transmission scheme under uniform puncturing (UP) pattern of Spinal codes with $n/k = 8$, puncturing sequence $\mathbf{g} = [g_1, g_2, \ldots, g_8] = [8, 7, 6, 5, 4, 3, 2, 1]$ where g_i represents the code symbol from the g_ith spine value in the ith sub-pass. Within a sub-pass in the UP pattern, only one symbol is transmitted as colored black, and the symbols that have been sent before are colored gray. For example, in sub-pass 4, if 2 passes of code symbols have been transmitted, the puncturing pattern can be denoted as $[2, 2, 2, 2, 3, 3, 3, 3]$. Note that in a more general transmission scheme, several sub-passes can be simultaneously transmitted in one round.

In addition to the transmission scheme under UP pattern, non-uniform puncturing pattern can also be used in the transmission scheme of Spinal codes, where the symbols from different spine values are transmitted unequally for different sub-passes (hence different puncturing sequences for different sub-passes). We can also use $\mathbf{L}_i$ to denote the puncturing pattern at round i.

In the transmission schemes with puncturing, a successful decoding can occur in any sub-pass. Note that although not all the code symbols of one pass are sent in the transmission scheme with puncturing, the decoding algorithm does not change. For the code symbols that are not sent in a certain sub-pass under certain puncturing pattern, the path cost of these nodes in the bubble decoding will be zero. For example, if the puncturing pattern is $[2, 2, 2, 2, 3, 3, 3, 3]$, then the path costs for the first four code symbols of pass 3 are zeros.

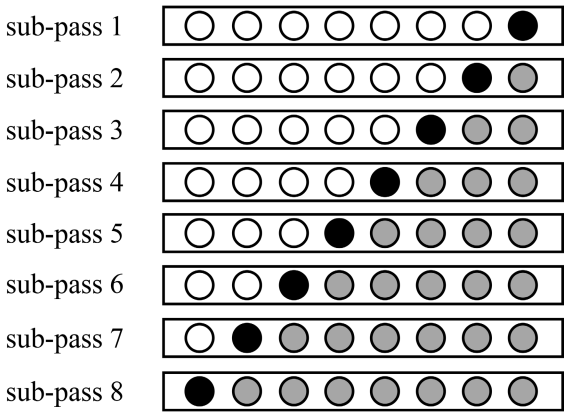

Fig. 2. A transmission scheme under UP pattern of Spinal codes with puncturing sequence $\mathbf{g} = [8, 7, 6, 5, 4, 3, 2, 1]$.

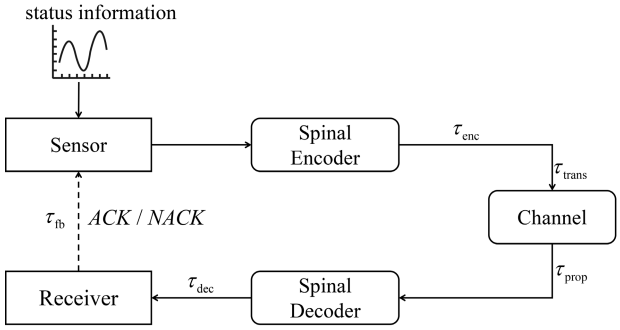

Fig. 3. The model of the HARQ-based Spinal coded system.

III. System Model

Consider an end-to-end HARQ-based Spinal coded status update system in Fig. 3. In this system, a sensor continuously captures the random status update information from the environment, and the Spinal encoder encodes the status information to code symbols, which are then stored in the buffer of the sender side. After that, several passes of code symbols are transmitted over the channel. At the receiver side, the symbols that has just been received are decoded by Spinal decoder, and the decoding outputs are stored in the receiver. If the decoding fails, a negative acknowledgement (NACK) feedback is sent to the sender side by the receiver. Instantly several extra code symbols stored in the buffer are incrementally transmitted under a certain transmission scheme, and the receiver decodes the new received symbols together with the previous symbols and gives feedback. We define the cycle of a transmission, a decoding process and a feedback as one round. In order to ensure lower transmission delay and higher timeliness, the number of the total rounds (also the number of total code symbols) is restricted to be no more than a certain integer. Once a status update gets decoded, the AoI of the system will be instantly updated as the age of this status update, and then an acknowledgement (ACK) feedback will be sent to the sensor, and a new status update will be captured. If decoding still fails after maximum rounds of transmission, an NACK will be sent to the sender, and still a new status update will be captured. In this paper, we focus on the line-of-sight (LOS) AWGN channel model.

A. Notations

We denote such HARQ transmission scheme $\mathcal{N} = [\nu_1, \nu_2, \ldots \nu_r]$ for a certain code. Under the transmission scheme $\mathcal{N}$, at the first round, ν_1 code symbols are transmitted over the channel, and if decoding fails at round i, then $\nu_{i+1} - \nu_i$ symbols are incrementally transmitted in the round $i+1$, until the decoding succeeds or the total number of rounds reaches r. We denote the delay as τ, and the specific kind of delay, for example, encoding delay as τ_{enc}. We denote the distance of the sender and the receiver as D, and the velocity of light v. We denote the instant AoI of the system as A, and the average AoI $\bar{A}$, respectively. We denote $\lceil \cdot \rceil$ as rounding up the numbers to integers.

For Spinal codes, we denote the transmission scheme as $\mathcal{N} = [(\nu_1, \mathbf{L}_1), (\nu_2, \mathbf{L}_2), \ldots, (\nu_r, \mathbf{L}_r)]$, where $\mathbf{L}_i = [l_{i,1}, l_{i,2}, l_{i,n/k}]$ is the puncturing pattern at round i, and $l_{i,j}$ represents the number of total code symbols that correspond to the jth spine value. We denote the status update information (message) length as n, the segmentation parameter as k, and the modulation parameter as c. If P passes of symbols are transmitted at the first round, then for Spinal codes with normal pass-by-pass transmission scheme we have $\nu_i = (P + i - 1) \cdot n/k, i = 1, 2, \ldots, r$, and for Spinal codes with transmission scheme under UP pattern we have $\nu_i = P \cdot n/k + i - 1, i = 1, 2, \ldots, r$. Denote the noise variance of the AWGN channel as σ^2, and the SNR as f. Denote the probability of successful decoding at round i as $P_s(\nu_i)$, and the error probability at round i as $P_e(\nu_i)$, so we have $P_s(\nu_i) = 1 - P_e(\nu_i)$. Also, we denote the transmission rate of Spinal codes as R. We assume that the channel is used once if one code symbol (including the feedback symbol ACK/NACK) is transmitted over the channel.

B. Delay and AoI Analysis of the HARQ-Based Spinal Coded System

Before we analyze the AoI of the system, we focus on the different types of delays in the transmission process because of its close connection with the age of the system. In this status update system, the following types of delays are considered, and note that all types of delays will be scaled by the channel use (CU) via the data rate R and rounded up as integers to study the symbol-level AoI.[1]

The AoI measures the time from the capture of the status update to the successful decoding of the same update, so the time of encoding process will increase the AoI. From the hardware perspective, the unit of a Spinal encoder is the hash-RNG module. We denote the clock cycle of the hash-RNG module (also the time of running this module once) as T_{hash}. Because of the sequential encoding structure, the encoding process of one message block costs one clock cycle of time. For Spinal codes with the message length n and the segmentation parameter k, the encoding delay is

$$\tau_{\text{enc}} = \lceil n/k \cdot T_{\text{hash}} \cdot R \rceil . \tag{2}$$

Note that the number of code symbols generated by RNG can be arbitrarily large because of the rate-variable characteristics of Spinal codes, so in the sending of one status update, the encoding process will only occur once in the first round, generating ν_r code symbols and storing them for the following rounds of transmission.

2) Transmission Delay: The transmission delay τ_{trans} is equal to the channel use C, namely the number of code symbols transmitted in the current round $\nu_i - \nu_{i-1}$, that is

$$\tau_{\text{trans}} = C = \nu_i - \nu_{i-1}. \tag{3}$$

[1]In the previous works about the AoI for channel coding [13], [14], [15], [16], the symbol-level AoI of the system is scaled by integer channel use.

3) Propagation Delay: In end-to-end communication and LOS scenario, the propagation delay is only the function of the distance between the sender and the receiver. Let the distance of the two end be D and the light speed v, then the one-way propagation delay of the system is

$$\tau_{\text{prop}} = \lceil D/v \cdot R \rceil . \tag{4}$$

Note that in both the transmission and the feedback, the propagation delay exists.

4) Decoding Delay: Usually the decoding delay plays a major role in the system because the complexity of decoding algorithm is much higher than the encoding process. Especially, in the practical application, the hardware source is sometimes limited, resulting in higher decoding delay. The Spinal bubble decoder consists of hash-RNG modules and sorting modules to reproduce the encoding process and sort the path cost of each candidate message, and the decoding delay is related to the time of running the two kinds of modules. Assuming that the pruning depth of the bubble decoder is B, and that the sorting algorithm will be executed once in each layer of the decoding tree, we analyze the decoding delay as below. Note that in this paper the time spent on the calculation of the path cost is so short that can be neglected.

In the ML decoding, in the ith layer of the decoding tree, the number of nodes will be $M_i = 2^{ki}, i = 1, 2, \ldots, n/k$. However, in the bubble decoding, only at most B nodes will remain after pruning. For the ith layer, the number of nodes depends on the number of nodes in the $(i-1)$th layer. If the number of the nodes in the $(i-1)$th layer is not greater than B, all the M_i nodes will be each spread into 2^k nodes. If not, the decoder will prune some nodes in the $(i-1)$th layer and only B nodes will be each spread into 2^k nodes. So the number of nodes in the ith layer in bubble decoding can be expressed as

$$\beta_i = \begin{cases} 2^k B & 2^{(i-1)k} > B, \\ 2^{ik} & 2^{(i-1)k} \le B. \end{cases} \tag{5}$$

We consider a parallel computing process with H hash-RNG modules in the bubble decoder. As such, H hash-RNG mapping processes can be simultaneously executed, so for β_i nodes, the number of times of hardware computing in the ith layer is

$$H_i = \begin{cases} \left\lceil \frac{2^k B}{H} \right\rceil & 2^{(i-1)k} > B, \\ \left\lceil \frac{2^{ik}}{H} \right\rceil & 2^{(i-1)k} \le B. \end{cases} \tag{6}$$

Assume that the quick sorting algorithm is applied in the sorting module with a time complexity $O(n \log n)$, then in the ith layer, β_i nodes will be sorted and the hash-RNG modules are used H_i times. Denote the clock cycle of the quick sorting algorithm as T_{sort}, then the total decoding delay is the sum of the delay of each layer, so the decoding delay is

$$\tau_{\text{dec}} = \left\lceil R \cdot \left(T_{\text{hash}} \cdot \sum_{i=1}^{n/k} H_i + T_{\text{sort}} \cdot \sum_{i=1}^{n/k} \beta_i \log_2 \beta_i \right) \right\rceil . \tag{7}$$

In our computer simulation of Spinal coded system, the time of running hash-RNG module once is approximately 10^{-5}, and the clock cycle of the sorting algorithm is approximately 10^{-8},

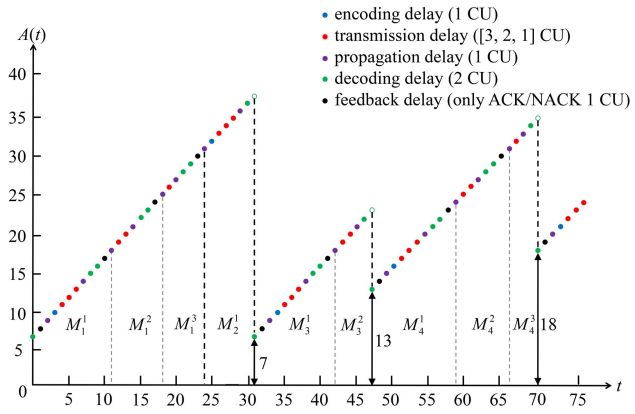

Fig. 4. The AoI evolution process of an HARQ-based status update system with a transmission scheme $\mathcal{N} = [3, 5, 6]$ for a certain code.

respectively, so we choose $T_{\text{hash}} = 10^{-5}$ and $T_{\text{sort}} = 10^{-8}$ in this paper unless otherwise specified.

5) Feedback Delay: After decoding, a 1-bit ACK or NACK will be sent back, using the channel once, and the bit will also experience the propagation delay, so the feedback delay is

$$\tau_{\text{fb}} = 1 + \tau_{\text{prop}}. \tag{8}$$

For the transmission scheme $\mathcal{N} = [\nu_1, \ldots, \nu_r]$, if a status update gets decoded, the AoI of the system will be updated as the age of this status update, that is $A = \tau_{\text{enc}} + \tau_{\text{trans}} + \tau_{\text{prop}} + \tau_{\text{dec}}$. Then, an ACK will be sent to the sender, which cost τ_{fb} CUs, and the sensor will capture the next status update. If a status update cannot be decoded by the receiver after r rounds of transmission, then an NACK feedback will be sent to the sender, and a new update will be generated with AoI continuously increasing.

Fig. 4 describes the AoI evolution process of an HARQ system with the transmission scheme of $\mathcal{N} = [3, 5, 6]$, with $\tau_{\text{enc}} = 1$, $\tau_{\text{prop}} = 1$, $\tau_{\text{dec}} = 2$, $\tau_{\text{fb}} = 1 + \tau_{\text{prop}} = 2$. In this process, four status updates are transmitted named M_1, M_2, M_3 and M_4, where M_i^j denotes the jth transmission round of the status update M_i. For M_1, after three rounds of transmission the decoding still fails and M_1 gets discarded. Then a new status update M_2 is encoded and transmitted. After a successful decoding at the first round, the AoI instantly gets updated as the age of M_2, namely $A = \tau_{\text{enc}} + \tau_{\text{trans}} + \tau_{\text{prop}} + \tau_{\text{dec}} = 7$ (here $\tau_{\text{trans}} = \nu_1 = 3$). After an ACK feedback, M_3 is encoded and transmitted and after two rounds M_3 gets successfully decoded, with the AoI of the system updated as 13. Then M_4 is transmitted and decoded within three rounds and the AoI is updated to 19 after M_4 gets successfully decoded.

IV. AoI Analysis of the HARQ-Based Spinal Coded Status Update System

A. The Average AoI of the HARQ-Based Spinal Coded System

In [14], the average AoI of the HARQ coded system considering only transmission delay is derived scaled by CU, with regard to the transmission scheme $\mathcal{N} = [\nu_1, \nu_2, \ldots \nu_r]$ and the successful decoding probability in each round $P_s(\nu_i), i = 1, 2, \ldots, r$, as the following expression.

$$\overline{A} = \frac{\mathbb{E}(T^2)}{2\mathbb{E}(T)} + \mathbb{E}(\nu_V) - \frac{1}{2}, \tag{9}$$

where

$$\begin{aligned}
\mathbb{E}(T) &= \frac{\nu_r}{P_s(\nu_r)} - \sum_{i=1}^{r-1} (\nu_{i+1} - \nu_i) \frac{P_s(\nu_i)}{P_s(\nu_r)}, \\
\mathbb{E}(T^2) &= \frac{\nu_r^2 (1 + \overline{P_s(\nu_r)})}{P_s(\nu_r)^2} \\
&\quad - \sum_{i=1}^{r-1} \frac{P_s(\nu_i)}{P_s(\nu_r)} (\nu_{i+1} - \nu_i)(\nu_{i+1} + \nu_i + 2\nu_r \frac{\overline{P_s(\nu_r)}}{P_s(\nu_r)}), \\
\mathbb{E}(\nu_V) &= \nu_r - \sum_{i=1}^{r-1} (\nu_{i+1} - \nu_i) \frac{P_s(\nu_i)}{P_s(\nu_r)},
\end{aligned} \tag{10}$$

where T represents the CU of one status information, and V represents the round in which the decoding succeeds.

In the HARQ-based coded system with different types of delays, for a newly generated status update, it will be encoded to code symbols by the encoder and ν_i code symbols are transmitted before round i, and if decoding fails, an NACK will be sent back to the encoder for next round. If decoding fails at round r, then an NACK will be sent back to generate next status update. We denote $\nu_i' = \nu_i + \tau_{\text{enc}} + i(\tau_{\text{prop}} + \tau_{\text{dec}} + \tau_{\text{fb}})$ as the equal channel use in each round, and γ as the number of the status updates that have failed in decoding before a successfully decoded status update, then we have $T = \gamma \nu_r' + \nu_V' - \tau_{\text{fb}}$. Note that there is a term of $-\tau_{\text{fb}}$ because when decoding succeeds the AoI instantly gets updated, and the feedback delay at the successful decoding round should be subtracted. It is easy to infer that γ obeys geometric distribution with $\mathbb{P}(\gamma = g) = (1 - P_s(\nu_m))^{g-1} \cdot P_s(\nu_m)$. Then by calculating $\mathbb{E}(T)$, $\mathbb{E}(T^2)$ and $\mathbb{E}(\nu_V)$ in (9) we have the AoI of the system with delays as follows, (11), as shown at the bottom of the next page, where $\tau_{\text{extra}} = 2\tau_{\text{prop}} + \tau_{\text{dec}} + \tau_{\text{fb}}$.

For Spinal codes with parameters n and k with normal pass-by-pass transmission scheme, at the first round P passes of code symbols are transmitted, and in each incremental round one pass of symbols are sent until a successful decoding or the total number of rounds reaches r. In this case we have $\nu_i = d(P + i - 1), i = 1, 2, \ldots, r$, where $d = n/k$ denotes the number of code symbols in a pass. By substituting ν_i into (11) we can derive the average AoI of the HARQ-based Spinal coded system with normal transmission scheme as shown in Theorem 1. For Spinal codes with transmission scheme under UP pattern, assume that only one symbol is transmitted in an incremental round, that is $\nu_i = dP + i - 1, i = 1, 2, \ldots, r$, where $d = n/k$. Similarly we can derive the average AoI of the HARQ-based Spinal coded system with transmission scheme under UP pattern in Theorem 2.

Theorem 1 (The Average AoI of the HARQ-Based Spinal Coded System With Normal Transmission Scheme): Consider the Spinal coded system with message length n and segmentation parameter k. At the first round, P passes of code symbols are transmitted and the maximum round is r, and let $d = n/k$,

then the average AoI with normal transmission scheme is, (12), as shown at the bottom of the page.

Proof: Please refer to Appendix A. □

Theorem 2 (The Average AoI of the HARQ-Based Spinal Coded System With Transmission Scheme Under UP Pattern): Consider the Spinal coded system with message length n and segmentation parameter k. At the first round, P passes of code symbols are transmitted and the maximum round is r, and let $d = n/k$, then the average AoI with transmission scheme under UP pattern is, (13), as shown at the bottom of the next page.

The proof of Theorem 2 is similar to Theorem 1. For other transmission schemes of Spinal codes, we can similarly get the number of code symbols in each round ν_i and substitute into (11) to derive the average AoI expression.

B. Monotony Analysis of the AoI Expression (11)

Although the average AoI is decreasing with the error probability intuitively, no previous work has studied the monotony of average AoI with error probability either numerically or theoretically, because the expression of average AoI is complex and difficult to analyze its monotony, as has been derived in (11). In this subsection we try to analyze the monotony of $\bar{A}$ with $P_s(\nu_i), i = 1, 2, \ldots, n/k$ based on some numerical simulations, to further give a bound for average AoI. Specifically, we can calculate the partial derivative of $\bar{A}$ in (11) with respect to $P_s(\nu_j)$ as, (14), shown at the bottom of the next page.

Though the sign of (14) can not be analytically derived, we can still validate the negativity of (14) under certain conditions by simulation in which we randomly choose ν_i, $P_s(\nu_i)$ such that $\nu_i < \nu_{i+1}$ and $P_s(\nu_i) < P_s(\nu_{i+1})$ to observe the value of the derivative. By our simulation we find out that when τ_{dec} and ν_r are of the same order of magnitude or $\tau_{\text{dec}} \gg \nu_r$, the partial derivative of (14) is always negative. Now we will choose some typical value of ν_r and τ_{dec}, with ν_i and $P_s(\nu_j)$ randomly generating, to show some simulation results of the value of $\frac{\partial \overline{A}}{\partial P_s(\nu_1)}$.

Fig. 5a shows the frequency distribution of the value of $\frac{\partial \overline{A}}{\partial P_s(\nu_1)}$, where $r = 5$, $\nu_r = 30$ and $\tau_{\text{dec}} = 16$. In this case, the decoding delay is close to the transmission delay. From Fig. 5a we can observe that the random variable $\frac{\partial \overline{A}}{\partial P_s(\nu_1)}$ is nearly uniformly distributed with negative values. Fig. 5b shows the frequency distribution of the value of $\frac{\partial \overline{A}}{\partial P_s(\nu_1)}$, where $r = 10$, $\nu_r = 120$ and $\tau_{\text{dec}} = 1000$. In this case, the decoding delay is much larger than the transmission delay. It is demonstrated by Fig. 5b that the probability distribution of the random variable $\frac{\partial \overline{A}}{\partial P_s(\nu_1)}$ has a peak value and is always negative.

From Fig. 5a and Fig. 5b we can conclude that the event that the average AoI in (11) is decreasing with $P_s(\nu_i)$ is always true under the condition that the decoding delay is

$$\begin{aligned}\bar{A} = {} & \frac{\nu_r + \tau_{\text{enc}} + r\tau_{\text{extra}} - \sum_{i=1}^{r-1}(\nu_{i+1} - \nu_i + \tau_{\text{extra}})P_s(\nu_i)}{P_s(\nu_r)} \\ & + \frac{(\nu_r + \tau_{\text{enc}} + r\tau_{\text{extra}})^2}{2(\nu_r + \tau_{\text{enc}} + r\tau_{\text{extra}} - \sum_{i=1}^{r-1}(\nu_{i+1} - \nu_i + \tau_{\text{extra}})P_s(\nu_i))} \\ & - \frac{\sum_{i=1}^{r-1}(\nu_{i+1} - \nu_i + \tau_{\text{extra}})(\nu_{i+1} + \nu_i + 2\tau_{\text{enc}} + \tau_{\text{extra}}(2i+1))P_s(\nu_i)}{2(\nu_r + \tau_{\text{enc}} + r\tau_{\text{extra}} - \sum_{i=1}^{r-1}(\nu_{i+1} - \nu_i + \tau_{\text{extra}}))P_s(\nu_i)} \\ & - \frac{1}{2} - \tau_{\text{fb}}, \end{aligned} \tag{11}$$

$$\begin{aligned}\bar{A} = {} & \frac{d(P + r - 1) + \tau_{\text{enc}} + r\tau_{\text{extra}} - \sum_{i=1}^{r-1}(d + \tau_{\text{extra}})P_s(\nu_i)}{P_s(\nu_r)} \\ & + \frac{(d(P + r - 1) + \tau_{\text{enc}} + r\tau_{\text{extra}})^2}{2(d(P + r - 1) + \tau_{\text{enc}} + r\tau_{\text{extra}} - \sum_{i=1}^{r-1}(d + \tau_{\text{extra}})P_s(\nu_i))} \\ & - \frac{\sum_{i=1}^{r-1}(d + \tau_{\text{extra}})((2P + 2i - 1)d + 2\tau_{\text{enc}} + \tau_{\text{extra}}(2i+1))P_s(\nu_i)}{2(d(P + r - 1) + \tau_{\text{enc}} + r\tau_{\text{extra}} - \sum_{i=1}^{r-1}(d + \tau_{\text{extra}})P_s(\nu_i))} \\ & - \frac{1}{2} - \tau_{\text{fb}}. \end{aligned} \tag{12}$$

close to or much larger than the transmission delay, which can be easily achieved in 5G wireless communications under the transmission rate of $R \approx 10^5$ to $R \approx 10^7$. Unless otherwise specified in this paper, in the analysis of average AoI upper bound and the simulation of average AoI, the condition of the decoding delay is always satisfied. [2]

C. The Average AoI Upper Bound of the HARQ-Based Spinal Coded System

By analyzing the monotony of $\frac{\partial \overline{A}}{\partial P_s(\nu_i)}$, we can further give the bound of $\bar{A}$. In [24] which is our previous work, we derive a tighter FER upper bound of Spinal codes over the AWGN channel. Note that the average AoI is decreasing with the probability of successful decoding, so the average AoI is increasing with the error probability (also the FER). By substituting the FER upper bound into (11) we can derive the average AoI upper bound of the HARQ-based Spinal coded system. We firstly give the FER upper bound of Spinal codes over the AWGN channel in the following lemma.

[2]For the situations where the decoding delay is small, the average AoI will not decrease with the successful decoding probability. We will consider this situation in our future work.

Lemma 1 (Our Previous Work in [24]) (Approximate FER Upper Bound for Spinal Codes Over the AWGN Channel): Consider Spinal codes with message length n, segmentation parameter k and modulation parameter c transmitted over the AWGN channel with noise variance σ^2. Let $\mathbf{L} = [l_1, l_2, \ldots, l_{n/k}]$ be the puncturing pattern of Spinal codes, then the FER under ML decoding can be approximately upper bounded by

$$P_e \leq 1 - \prod_{i=1}^{n/k}(1-\epsilon_i), \tag{15}$$

with

$$\epsilon_i = \min\left\{1, \left(2^k - 1\right) 2^{n-ik} \cdot \min\left(1, R_i\right)\right\}, \tag{16}$$

where

$$R_i = \frac{1}{\Gamma\left(1+N_i \Big/ 2\right)} \left(\frac{\pi \sigma^2 N_i}{2^{2c}}\right)^{N_i \Big/ 2}, \tag{17}$$

where $\Gamma(\cdot)$ denotes the Gamma function, $N_i = \sum_{j=i}^{n/k} l_j$.

From Lemma 1 we know that P_e is related to the puncturing pattern in each round. Given the transmission scheme

$$\begin{aligned}\bar{A} = &\frac{Pd + r - 1 + \tau_{\text{enc}} + r\tau_{\text{extra}} - \sum_{i=1}^{r-1}(1+\tau_{\text{extra}})P_s(\nu_i)}{P_s(\nu_r)} \\ &+ \frac{\left(Pd + r - 1 + \tau_{\text{enc}} + r\tau_{\text{extra}}\right)^2}{2(Pd + r - 1 + \tau_{\text{enc}} + r\tau_{\text{extra}} - \sum_{i=1}^{r-1}(1+\tau_{\text{extra}})P_s(\nu_i))} \\ &- \frac{\sum_{i=1}^{r-1}(1+\tau_{\text{extra}})(2Pd + 2i - 1 + 2\tau_{\text{enc}} + \tau_{\text{extra}}(2i+1))P_s(\nu_i)}{2(Pd + r - 1 + \tau_{\text{enc}} + r\tau_{\text{extra}} - \sum_{i=1}^{r-1}(1+\tau_{\text{extra}})P_s(\nu_i))} \\ &- \frac{1}{2} - \tau_{\text{fb}}.\end{aligned} \tag{13}$$

$$\begin{aligned}\frac{\partial \overline{A}}{\partial P_s(\nu_j)} = &\frac{-(\nu_{j+1} - \nu_j) - \tau_{\text{extra}}}{P_s(\nu_r)} \\ &+ \frac{(\nu_r + \tau_{\text{enc}} + r\tau_{\text{extra}})^2(\nu_{j+1} - \nu_j + \tau_{\text{extra}})}{2(\nu_r + \tau_{\text{enc}} + r\tau_{\text{extra}} - \sum_{i=1}^{r-1}(\nu_{i+1} - \nu_i + \tau_{\text{extra}})P_s(\nu_i))^2} \\ &- \frac{(\nu_{j+1} - \nu_j + \tau_{\text{extra}})((\nu_{j+1} + \nu_j + 2\tau_{\text{enc}} + \tau_{\text{extra}}(2j+1))}{2(\nu_r + \tau_{\text{enc}} + r\tau_{\text{extra}} - \sum_{i=1}^{r-1}(\nu_{i+1} - \nu_i + \tau_{\text{extra}})P_s(\nu_i))^2} \\ &\cdot(\nu_r + \tau_{\text{enc}} + r\tau_{\text{extra}} - \sum_{i=1}^{r-1}(\nu_{i+1} - \nu_i + \tau_{\text{extra}})P_s(\nu_i)) \\ &- \frac{(\nu_{j+1} - \nu_j + \tau_{\text{extra}})^2 \sum_{i=1}^{r-1}(\nu_{i+1} + \nu_i + 2\tau_{\text{enc}} + \tau_{\text{extra}}(2i+1))P_s(\nu_i)}{2(\nu_r + \tau_{\text{enc}} + r\tau_{\text{extra}} - \sum_{i=1}^{r-1}(\nu_{i+1} - \nu_i + \tau_{\text{extra}})P_s(\nu_i))^2}.\end{aligned} \tag{14}$$

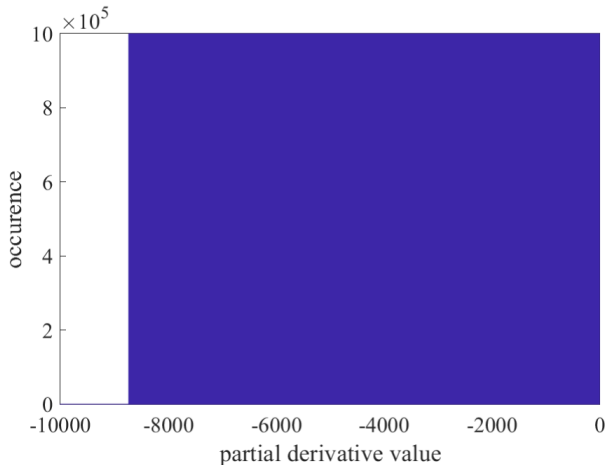

(a) $r = 5$, $\nu_r = 30$ and $\tau_{\text{dec}} = 16$.

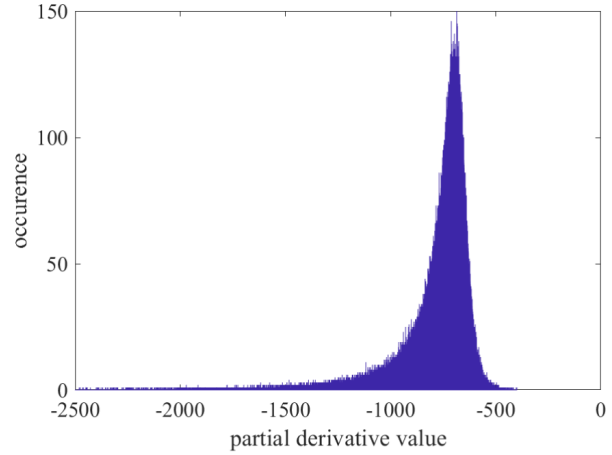

(b) $r = 10$, $\nu_r = 120$ and $\tau_{\text{dec}} = 1000$.

Fig. 5. The frequency distribution histogram of $\frac{\partial \overline{A}}{\partial P_s(\nu_1)}$ with different parameters.

$\mathcal{N} = [(\nu_1, \mathbf{L}_1), (\nu_2, \mathbf{L}_2), \ldots, (\nu_r, \mathbf{L}_r)]$, we can calculate the FER upper bound in each round by substituting $\mathbf{L}_i$ into (15). We denote the FER upper bound at round i by $P_e^{\text{upper}}(\nu_i)$. Because $P_s(\nu_i) = 1 - P_e(\nu_i)$, we have the lower bound of the probability of successful decoding is $P_s^{\text{lower}}(\nu_i) = 1 - P_e^{\text{upper}}(\nu_i)$. Because the average AoI is decreasing with $P_s(\nu_i)$, we can derive the average AoI upper bound for the HARQ-based Spinal coded system over the AWGN channel $\bar{A}^{\text{upper}}$ by substituting $P_s^{\text{lower}}(\nu_i)$ into the average AoI expression in (11), as shown in the following theorem.

Theorem 3 (The Average AoI Upper Bound for the HARQ-Based Spinal Coded System Over the AWGN Channel Under Certain Puncturing Pattern): Consider the HARQ-based Spinal coded system with status information length n, segmentation parameter k, and the transmission scheme $\mathcal{N} = [(\nu_1, \mathbf{L}_1), (\nu_2, \mathbf{L}_2), \ldots, (\nu_r, \mathbf{L}_r)]$. Let $P_s^{\text{lower}}(\nu_i) = 1 - P_e^{\text{upper}}(\nu_i)$ be the lower bound of probability of successful decoding at round i which can be calculated by (15), then the average AoI of the system can be upper bounded by, (18), as shown at the bottom of the next page.

In section V, the average AoI upper bound will be utilized as the objective function to optimize the transmission scheme for the HARQ-based Spinal coded system.

V. AoI Optimization of the HARQ-Based Spinal Coded System

In this section, we aim to optimize the puncturing pattern and the number of code symbols in each round to construct an Spinal coded HARQ transmission scheme with minimum AoI, under the constraint of the number of total incremental redundancy symbols. Although the objective function is the average AoI upper bound in (18) instead of the real average AoI, we can still find out the best transmission scheme, for lower AoI upper bound implies lower real average AoI. The transmission scheme consists of two degree of freedom, and directly taking the whole transmission scheme as the decision variable will cause extremely high computing complexity. Therefore, we separate the optimization algorithm of the transmission scheme into two steps to simplify the problem. Firstly, in order to find the best puncturing position for each incremental symbol, we first optimize the puncturing pattern under a symbol-by-symbol transmission scheme. Using the optimal puncturing pattern we have just solved, we can then optimize the number of code symbols in each incremental round to find the best allocation of symbols. Combining the two solutions to the two problems, we can finally get the optimal transmission scheme.

A. HARQ Transmission Scheme Optimization Under the Most Fine-Grained Puncturing Pattern

Firstly, we try to optimize the puncturing pattern in each round. In other words, the purpose of this step is to find out transmitting which symbol will achieve the lowest AoI in each round. As a result, we consider a transmission scheme where the transmission process is symbol by symbol. That is, after transmitting several passes of symbols at the first round, the transmitter sends only one encoded symbol in each incremental transmission round with the number of total incremental symbols equal to $I_{\max}$. We define such symbol-by-symbol transmission scheme as the transmission scheme under the most fine-grained puncturing pattern. The goal of this optimization is to find the best puncturing position in each round for Spinal coded system to get lowest AoI.

For Spinal codes with message length n and segmentation parameter k, the AoI minimization problem can be expressed as follows:

1) **Objective function**: The average AoI upper bound A^{upper}, which is denoted by (18). Although the average AoI upper bound is not the real average AoI, we can still choose A^{upper} as the objective function, because minimizing the upper bound will lead to lower real average AoI than the corresponding upper bound, which also achieves our goal.

2) **Decision variables**: The number of symbols from each spine value, namely the puncturing pattern $\mathbf{L}_i = [l_{i,1}, l_{i,2}, \ldots, l_{i,n/k}]$ at round $i, i = 1, 2, \ldots, r$. In this case, the transmission scheme is $\mathcal{N} = [(\nu_1, \mathbf{L}_1), (\nu_2, \mathbf{L}_2), \ldots, (\nu_r, \mathbf{L}_r)]$, where ν_i is the sum of the elements of the vector $\mathbf{L}_i$, and $\nu_i - \nu_{i-1} = 1$ for $i \geq 2$. We assume that $\nu_1 = nP/k$ and $\mathbf{L}_1 = [P, P, \ldots, P]$, that is, P passes of code symbols are transmitted in the first round.

3) **Constraint**: The number of incremental symbols is equal to $I_{\max}$. In fact, the constraint is equal to the restriction of the number of total code symbols when ν_1 is fixed.

To sum up, the overall optimization problem can be formulated as follows.

Problem 1: The AoI minimization problem for the transmission scheme under the most fine-grained puncturing pattern:

$$\begin{aligned} \min \quad & A^{\text{upper}} \\ s.t. \quad & c_1 : l_{i,1}, l_{i,2}, \ldots, l_{i,n/k} \in Z^+ \quad \text{for} \quad i = 1, 2, \ldots, n/k, \\ & c_2 : \nu_r - \nu_1 = I_{\max}. \end{aligned} \tag{19}$$

where A^{upper} can be calculated by (18).

Note that Problem 1 is an integer programming problem, and can be solved by exhausting algorithm when $I_{\max}$ is small. But for large $I_{\max}$, the exhausting algorithm cannot be executed in limited time. Instead, we design a dynamic iteration algorithm based on the tree structure to solve this integer programming problem, similar to the bubble decoding algorithm of Spinal codes. In each iteration round (also the transmission round), one candidate symbol is transmitted, with the nodes in the current layer spread to construct a n/k-ary tree, whose nodes represent the candidate puncturing patterns. Only β nodes with the least AoI upper bound will remain. When the total number of incremental symbols is $I_{\max}$, the algorithm ends with an output of the optimal decision value, namely the optimal puncturing patterns in each round. Specifically, the iteration algorithm is elaborated in Algorithm 1.

Note that in Algorithm 1, the AoI upper bound can be calculated by (18) considering the transmission scheme until the current layer (or the current round) based on the node path from the root node to a certain child node. For example, if the current round is the third round, then the transmission scheme is $[(\nu_1, \mathbf{L}_1), (\nu_1 + 1, \mathbf{L}_2), (\nu_1 + 2, \mathbf{L}_3)]$. Solving Problem 1 by the algorithm above with $n = 32$, $k = 4$, $P = 3$, $R = 10^5$, $B = 64$, $H = 64$, $D = 0$,[3] and $\beta = 4$, the results are shown in Table I. Here only the puncturing pattern in the last round is shown. The reason is that in every round before the last round, the solution is also transmitting the symbol from the n/kth spine value, forming the same transmission scheme.

[3]By our simulation, these variables do not affect the final solutions.

Algorithm 1 The Optimal Transmission Scheme Under the Most Fine-Grained Puncturing Pattern for the HARQ-Based Spinal Coded System

Input: Message length n; segmentation parameter k; puncturing pattern at the first round $\mathbf{L}_1 = [l_1, l_2, \ldots, l_{n/k}]$ where $l_1 = \ldots = l_{n/k} = P$; transmission round $r = 1$; the SNR f, the distance D; the maximum number of incremental code symbols $I_{\max}$; transmission rate R, pruning depth B and the number of parallel hash module H.

Output: The optimal puncturing pattern with the least AoI upper bound.

Initialize root node $c_{1,1}$ by the puncturing pattern $\mathbf{L}_1$;
while $r \leq I_{\max} + 1$ **do**
  Transmit a code symbol: the transmission round $r = r + 1$;
  Spread the nodes in the rth layer . Specifically, for each father node $c_{r-1,j}, j = 1, 2, \ldots, \min\{(n/k)^{r-1}, \beta\}$, n/k candidate symbols at each puncturing position are transmitted to generate node $c_{r,j}, j = 1, \ldots, n/k$ containing a puncturing pattern of current round $\mathbf{L}_r = \mathbf{L}_{r-1}$;
  For node $c_{r,j}$ in the rth layer, the puncturing pattern in the current round $\mathbf{L}_r$ gets updated: $l_{r,j} = l_{r,j} + 1$;
  For each child node $c_{r,j}$, calculate the AoI upper bound $\bar{A}_{r,j}^{\text{upper}}$ under the SNR f based on the transmission scheme $[(Pn/k, \mathbf{L}_1), (Pn/k+1, \mathbf{L}_2), \ldots, (Pn/k+r-1, \mathbf{L}_r)]$;
  if *the number of nodes* $> \beta$ **then**
    β nodes with least AoI upper bound $c_{r,j}, j = 1, 2, \ldots, \beta$ will remain and be spread in the next cycle;
return The optimal node path, i.e. the puncturing pattern in each round or the transmission scheme.

From Table I, we can find out that the puncturing pattern in the last round (also in each round obviously) forms the most fine-grained incremental-tail-transmission puncturing pattern (ITTP pattern) for the transmission scheme, which means that

$$\begin{aligned} \overline{A^{\text{upper}}} = & \frac{\nu_r + \tau_{\text{enc}} + r\tau_{\text{extra}} - \sum_{i=1}^{r-1} (\nu_{i+1} - \nu_i + \tau_{\text{extra}}) P_s^{\text{lower}}(\nu_i)}{P_s^{\text{lower}}(\nu_r)} \\ & + \frac{(\nu_r + \tau_{\text{enc}} + r\tau_{\text{extra}})^2}{2(\nu_r + \tau_{\text{enc}} + r\tau_{\text{extra}} - \sum_{i=1}^{r-1} (\nu_{i+1} - \nu_i + \tau_{\text{extra}}) P_s^{\text{lower}}(\nu_i))}. \\ & - \frac{\sum_{i=1}^{r-1} (\nu_{i+1} - \nu_i + \tau_{\text{extra}})(\nu_i + \nu_{i+1} + 2\tau_{\text{enc}} + \tau_{\text{extra}}(2i+1)) P_s^{\text{lower}}(\nu_i)}{2(\nu_r + \tau_{\text{enc}} + r\tau_{\text{extra}} - \sum_{i=1}^{r-1} (\nu_{i+1} - \nu_i + \tau_{\text{extra}}) P_s^{\text{lower}}(\nu_i))} \\ & - \frac{1}{2} - \tau_{\text{fb}}. \end{aligned} \tag{18}$$

TABLE I
THE OPTIMAL PUNCTURING PATTERN WITH DIFFERENT NUMBER OF INCREMENTAL SYMBOLS $I_{\max}$

$I_{\max}$	**The optimal puncturing pattern in the last round $\mathbf{L}_r$**
6	$\mathbf{L}_r = [3,3,3,3,3,3,3,9]$
9	$\mathbf{L}_r = [3,3,3,3,3,3,3,12]$
12	$\mathbf{L}_r = [3,3,3,3,3,3,3,15]$
15	$\mathbf{L}_r = [3,3,3,3,3,3,3,18]$

in each incremental round continuously transmitting the coded symbols from the n/kth spine value will lead to lower AoI. In other words, ITTP pattern is the best puncturing pattern that achieves higher timeliness. Also, if there are restricts for Spinal codes in Algorithm 1 that the whole pass must be transmitted before transmitting the symbols from the next pass, we can also get the solution that the optimal uniform puncturing pattern for the HARQ-based Spinal coded system is inverse uniform puncturing pattern, where the symbols from the n/kth spine value is firstly transmitted, and the symbols from the $(n/k-1)$th spine value the second and so on, as the puncturing pattern in Fig. 2. Unless otherwise specified, in the simulation of HARQ Spinal coded system with transmission scheme under UP pattern, inverse UP pattern is utilized as a default.

B. HARQ Transmission Scheme Optimization Under Coarse-Grained Puncturing Pattern

After getting the best puncturing pattern, we focus on the symbol allocation in each transmission round to construct the best transmission scheme. Therefore, we consider a more general transmission scheme where more than one code symbols instead of one symbol are transmitted in the incremental rounds. Again, we define such transmission scheme as the transmission scheme under coarse-grained puncturing pattern. Although the transmission scheme under the most fine-grained ITTP pattern is the optimal symbol-by-symbol transmission scheme, ITTP pattern may not outperform coarse-grained puncturing pattern in the aspect of AoI, especially when the decoding delay is large. For example, if the code symbols are transmitted one by one at the first few rounds, though the transmission delay is reduced, the probability of decoding failure may be high due to the small number of code symbols. In this case, each round of failed decoding will cause a large AoI growth because of large decoding delay. Nevertheless, if several code symbols instead of one symbol are transmitted at the first few rounds, these code symbols may greatly increase the probability of successful decoding in these rounds, decreasing the average AoI of the system. Therefore, it is necessary to further study the transmission scheme under coarse-grained puncturing pattern.

In this subsection, we aim to find a transmission scheme under coarse-grained puncturing pattern that minimizes the AoI of the system under the constraint of total number of incremental code symbols. Because the transmission scheme under ITTP pattern is the optimal transmission scheme under the most fine-grained puncturing pattern, in this subsection, only the tail symbols are transmitted, which significantly simplifies the problem.

For Spinal codes with message length n and segmentation parameter k, the AoI optimization problem under coarse-grained puncturing pattern can be expressed as follows:

1) **Objective function**: The AoI upper bound A^{upper}, which is denoted by (18). Note that for the transmission scheme under non-uniform puncturing pattern we can only use (18) to calculate the AoI upper bound.

2) **Decision variables**: The transmission scheme $[(\nu_1, \mathbf{L}_1), (\nu_2, \mathbf{L}_2), \ldots, (\nu_r, \mathbf{L}_r)]$. In the incremental rounds, $\nu_{i+1} - \nu_i$ tail symbols will be transmitted to form the puncturing patterns of $\mathbf{L}_1 = [l_1, \ldots, l_{n/k}]$ at round 1 and $\mathbf{L}_i = [l_1, \ldots, l_{n/k} + \nu_{i+1} - \nu_1], i \geq 2$ at round i, respectively. We define this transmission scheme as the transmission scheme under coarse-grained ITTP pattern.

3) **Constraint**: The number of incremental symbols is equal to $I_{\max}$, with $\nu_r = \nu_1 + I_{\max}$.

The optimization problem can be formulated as follows:

Problem 2: The AoI minimization problem for the transmission scheme under coarse-grained ITTP pattern:

$$\begin{aligned} \min \quad & A^{\text{upper}} \\ s.t. \quad & c_1 : \nu_1, \nu_2, \ldots, \nu_t \in Z^+, \\ & c_2 : \nu_r - \nu_1 = I_{\max}, \end{aligned} \tag{20}$$

where A^{upper} can be calculated by (18).

Problem 2 is also an integer programming problem, and the key of solving it is to list all the transmission scheme $\mathcal{N}$. We divide the algorithm of the derivation of the transmission scheme list into two steps. Firstly we decompose $I_{\max}$ into the sum of a series of positive integers, for example, when $I_{\max} = 4$, the solutions are $4 = 1+1+1+1, 4 = 1+1+2, 4 = 1+3, 4 = 2+2, 4 = 4$. Secondly, we rearrange each of the series to do the full permutation for each case, for example, when $I_{\max} = 4$, the result of full permutation is the set of the following vectors $[1,1,1,1], [1,1,2], [1,2,1], [2,1,1], [1,3], [3,1], [2,2], [4]$, which can be used to derive the candidate decision variables, for example, the transmission scheme for the permutation of $[1,1,2]$ is $\mathcal{N} = [\nu_1, \nu_1+1, \nu_1+2, \nu_1+4]$. After calculating the AoI upper bound for each transmission scheme, the decision variable that has minimum AoI upper bound is the solution of the problem. The algorithm to the Problem 2 is detailed in Algorithm 2.

By algorithm 2 we solve the problem 2 under the condition of $n = 32$, $k = 4$, $P = 2$ ($\nu_1 = 16$), $R = 10^5$, $B = 64$, $H = 64$, $D = 0$,[4] $I_{\max} = 8$ and the SNR ranges from 10 dB to 20 dB, and the solutions can be seen in Table II. We also solve the problem under the condition of $R = 10^6$ with the other parameters same as those in Table II, and the solutions are elaborated in table III. The SNRs in Table II and Table III are accurate to two decimal places. It is demonstrated from Table II and Table III that the optimal decision values form

[4]In this paper, the terrestrial communication scenario is considered with small propagation delay that can be neglected, so we set $D = 0$ to represent the neglected propagation delay. The analysis and optimization of the system with large propagation delay can be extended following this work.

Algorithm 2 The Optimal Transmission Scheme Under Coarse-Grained ITTP Pattern for the HARQ-Based Spinal Coded System

Input: Message length n; segmentation parameter k; puncturing pattern $\mathbf{L} = [l_1, l_2, \ldots, l_{n/k}]$, and $l_1 = \ldots = l_{n/k} = P$; the SNR f, the distance D; the maximum number of incremental symbols $I_{\max}$; transmission rate R, pruning depth B and the number of parallel hash module H.

Output: The optimal transmission scheme with the least AoI upper bound.

Decompose $I_{\max}$ into the sum of a series of positive integers;

Rearrange each of the series to do the full permutation to generate all the candidate transmission scheme $\mathcal{N}_a$;

for $\mathcal{N}_a$ **do**

  Calculate the AoI upper bound $\bar{A}_a$ under the SNR f using equation (11) ;

Search for the minimum of $\bar{A}_a$ and get the index d;

return The optimal transmission scheme $\mathcal{N}_d$.

TABLE II

THE OPTIMAL TRANSMISSION SCHEME UNDER COARSE-GRAINED ITTP PATTERN WITH $n = 32$, $k = 4$, $R = 10^5$

SNR	The optimal decision variables $\mathcal{N}$
10-11.47 dB	$\mathcal{N} = [16, 24]$
11.48-11.85 dB	$\mathcal{N} = [16, 23, 24]$
11.86-12.51 dB	$\mathcal{N} = [16, 22, 24]$
12.52-13.46 dB	$\mathcal{N} = [16, 21, 24]$
13.47-15.81 dB	$\mathcal{N} = [16, 20, 24]$
15.82-20 dB	$\mathcal{N} = [16, 19, 22, 24]$
...	...

TABLE III

THE OPTIMAL TRANSMISSION SCHEME UNDER COARSE-GRAINED ITTP PATTERN WITH $n = 32$, $k = 4$, $R = 10^6$

SNR	The optimal decision variables $\mathcal{N}$
10-12.52 dB	$\mathcal{N} = [16, 24]$
12.53-13.08 dB	$\mathcal{N} = [16, 23, 24]$
13.09-14.30 dB	$\mathcal{N} = [16, 22, 24]$
14.31-16.90 dB	$\mathcal{N} = [16, 21, 24]$
16.91-20 dB	$\mathcal{N} = [16, 20, 24]$
...	...

a threshold structure. Specifically, when the SNR reaches a certain threshold, the optimal transmission scheme $\mathcal{N}$ changes in the aspect of the number of incremental tail symbols in each round and the number of total transmission round. Also, with the channel condition becoming better, the optimal transmission scheme is more close to the transmission scheme under the most fine-grained ITTP pattern in each round.

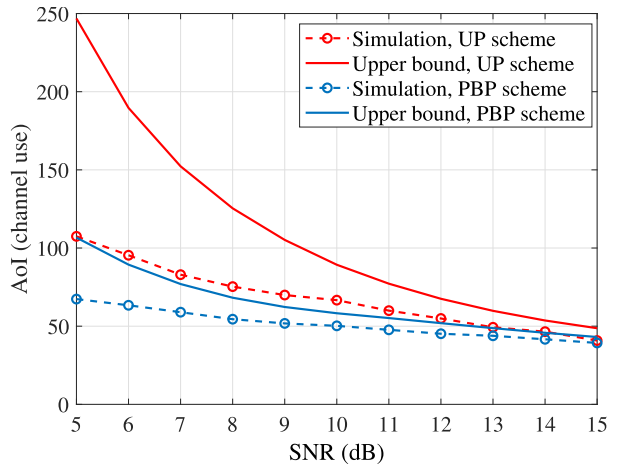

(a) $n = 8$, $k = 2$, $R = 10^5$.

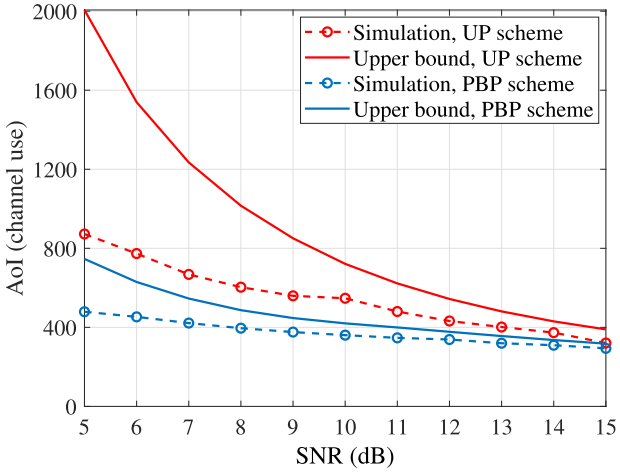

(b) $n = 8$, $k = 2$, $R = 10^6$.

Fig. 6. The simulation results and upper bound of AoI for the HARQ-based Spinal coded system with normal pass-by-pass transmission scheme and transmission scheme under UP pattern by bubble decoding with $B = 256$.

VI. NUMERICAL RESULTS

A. Average AoI Upper Bound of the HARQ-Based Spinal Coded System

Fig. 6a shows the simulation results and the upper bound in (18) of AoI of the HARQ-based Spinal coded system over the AWGN channel with normal pass-by-pass transmission scheme (PBP scheme) and transmission scheme under UP pattern (UP scheme), where $n = 8$, $k = 2$, $c = 8$, $R = 10^5$, $B = 256$, $H = 64$, $D = 0$ and at the first round one pass of code symbols are transmitted. For normal transmission scheme the maximum round is $r = 8$, so in the 8th round 8 passes of code symbols are transmitted; and for transmission scheme under UP pattern the maximum round is $r = 29$, so in the 29th round also 8 passes of code symbols are transmitted. Note that in this case the bubble decoding algorithm with $B = 256$ is equal to ML decoding, because in the n/kth layer the number of total nodes is 256, and no pruning is operated in bubble decoding, so the AoI upper bound derived in (18) can still be applied here to compare with the simulation results. With these parameters, we can calculate the encoding delay and decoding delay in the system, which are $\tau_{\text{enc}} = 4$, $\tau_{\text{dec}} = 10$. It can be seen from Fig. 6a that the both the AoI simulation and its

upper bound are decreasing as the channel condition becomes better. Besides, it is obvious that the AoI upper bound is tighter with the AoI simulation when the SNR is high in this case. Moreover, the AoI simulation and upper bound of transmission scheme under UP pattern are much higher than that of normal transmission scheme, for more rounds are experienced in the transmission of incremental puncturing symbols, which causes higher decoding delay.

Fig. 6b shows the simulation result and the upper bound in (18) of AoI of the HARQ-based Spinal coded system over the AWGN channel with normal transmission scheme and transmission scheme under UP pattern, where $R = 10^6$ and the other parameters are the same as those in Fig. 6a. In this case, the encoding delay and decoding delay are $\tau_{\text{enc}} = 40$ and $\tau_{\text{dec}} = 96$, which are much higher than the transmission delay. Specifically, compared to Fig. 6a, the AoI upper bound and simulation results under $R = 10^6$ are nearly eight times larger than those under $R = 10^5$, for the AoI of the system mainly depends on the encoding delay and decoding delay, and in this case the two types of delays are nearly ten times those under $R = 10^5$.

B. AoI Simulation of the HARQ-Based Spinal Coded System With the Optimal Transmission Scheme

Fig. 7a compares the AoI of the HARQ-based Spinal coded system with transmission scheme under the most fine-grained UP pattern [17] (UP scheme), ITTP pattern (ITTP scheme) and with the proposed optimal transmission scheme under coarse-grained ITTP pattern shown in Table II (Optimal scheme), where $n = 32$, $k = 4$, $B = 64$, $H = 64$, $R = 10^5$, $D = 0$, the maximum number of incremental symbols $I_{\max} = 8$ and at the first round two passes of code symbols are transmitted. In this case, the encoding delay and decoding delay are $\tau_{\text{enc}} = 8$ and $\tau_{\text{dec}} = 165$, respectively, and the maximum transmission delay is $\tau_{\text{trans}} = 24$. Clearly, the AoI of the system with the transmission scheme under the most fine-grained UP puncturing pattern is the highest, because the decoding delay is higher than the transmission delay and plays the main role in the AoI increase. In contrast, the transmission scheme under the most fine-grained ITTP pattern can reduce the AoI apparently, for the tail symbols increase the probability of successful decoding in the incremental rounds to improve the timeliness.

As for the optimal transmission scheme under coarse-grained ITTP pattern, the decrease of the AoI compared to the transmission scheme under the most fine-grained ITTP pattern should be analyzed from two aspects. On the one hand, at low SNR, the AoI of the optimal scheme is significantly lower than the transmission scheme under ITTP pattern, because the total number of rounds is much lower than ITTP pattern in average, resulting in smaller decoding delay in the system. On the other hand, at high SNR, the AoI of the optimal scheme is close to that of ITTP pattern, because the decoding can succeed at the first few rounds for both the two transmission schemes under more reliable channel condition, and in average the decoding delay under the two transmission schemes are closer, resulting in the small difference of AoI.

Fig. 7b compares the AoI of the HARQ-based Spinal coded system with transmission scheme under the most fine-grained UP pattern, ITTP pattern and with the proposed optimal transmission scheme under coarse-grained ITTP pattern shown in Table III, where $R = 10^6$ and the other parameters remain the same as those in Fig. 7a. In this case the encoding delay and decoding delay are $\tau_{\text{enc}} = 80$ and $\tau_{\text{dec}} = 1646$. With so large decoding delay, the other types of delays in the system can be nearly neglected, so the AoI is mainly affected by the decoding delay in each transmission round. Specifically, compared to Fig. 7a, the AoI under three transmission schemes with $R = 10^6$ are approximately ten times, for the decoding delay here is ten times that of the case with $R = 10^5$.

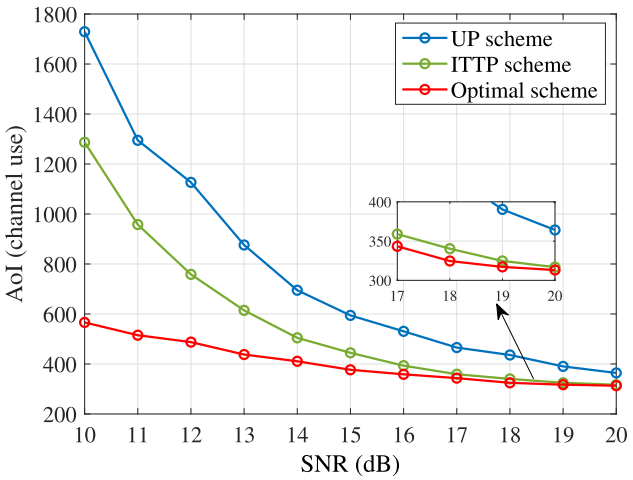

(a) $n = 32$, $k = 4$, $R = 10^5$.

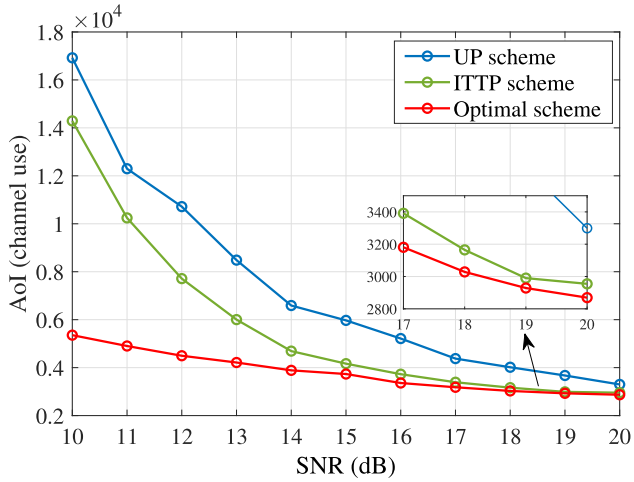

(b) $n = 32$, $k = 4$, $R = 10^6$.

Fig. 7. The AoI comparison of the transmission scheme under fine-grained UP pattern, ITTP pattern and the proposed optimal transmission scheme under coarse-grained puncturing pattern for the HARQ-based Spinal coded system.

VII. Conclusion and Future Work

In this paper, the Spinal coded timely status update system with HARQ transmission scheme is firstly analyzed. We analyze all the delay elements from the encoding, transmission, propagation, decoding and feedback process of the HARQ-based status update system, and we further observe the AoI evolution of the system. We theoretically derive the average AoI upper bound of the HARQ-based Spinal coded system. Utilizing the average AoI upper bound as the objective function, we formulate and solve the optimization problems

aimed at the HARQ transmission scheme of Spinal coded system, and propose the optimal transmission scheme under coarse-grained ITTP pattern. Simulation results demonstrate the superiority of the proposed optimal transmission scheme in the aspect of AoI compared to the transmission schemes under the most fine-grained puncturing patterns.

This paper provides an example of analyzing the average AoI of the HARQ-based coded status update system with different types of delays. For the system coded by other channel codes, similar ideas can be adopted to analyze the delay elements, AoI evolution processes and average AoI expressions considering the coding scheme and the FER or block error rate (BLER) of corresponding channel codes.

Appendix A
Proof of Theorem 1

Substitute ν_i' into (10) considering that at round V the AoI is updated instantly with no feedback (the total number of feedback delays for a successful frame is $V-1$), we have

$$\begin{aligned}
&\mathbb{E}(T)\\
&= \frac{(P+r-1)d+\tau_{\text{enc}}+r\tau_{\text{extra}}}{P_s(\nu_r)} - (d+\tau_{\text{extra}})\frac{\sum_{i=1}^{r-1}P_s(\nu_i)}{P_s(\nu_r)}\\
&= \frac{(P+r-1)d+\tau_{\text{enc}}+r\tau_{\text{extra}} - (d+\tau_{\text{extra}})\sum_{i=1}^{r-1}P_s(\nu_i)}{P_s(\nu_r)},
\end{aligned} \tag{21}$$

$$\begin{aligned}
&\mathbb{E}(T^2)\\
&= \frac{[\nu_r+\tau_{\text{enc}}+r\tau_{\text{extra}}]^2(2-P_s(\nu_r))}{{P_s}^2(\nu_r)}\\
&\quad -\sum_{i=1}^{r-1}\{\frac{P_s(\nu_i)}{P_s(\nu_r)}(d+\tau_{\text{extra}})[(2P+2i-1)d+2\tau_{\text{enc}}+(2i+1)\tau_{\text{extra}}\\
&\quad +2((P+r-1)d+\tau_{\text{enc}}+r\tau_{\text{extra}})\frac{1-P_s(\nu_r)}{P_s(\nu_r)}]\}\\
&= \frac{2[(P+r-1)+\tau_{\text{enc}}+r\tau_{\text{extra}}]^2}{{P_s}^2(\nu_r)}\\
&\quad -\frac{\sum_{i=1}^{r-1}(d+\tau_{\text{extra}})P_s(\nu_i)\cdot 2[(P+r-1)d+\tau_{\text{enc}}+r\tau_{\text{extra}}]}{{P_s}^2(\nu_r)}\\
&\quad -\frac{[(P+r-1)d+\tau_{\text{enc}}+r\tau_{\text{extra}}]^2}{P_s(\nu_r)}\\
&\quad +\frac{\sum_{i=1}^{r-1}(d+\tau_{\text{extra}})^2P_s(\nu_i)(2r-2i-1)}{P_s(\nu_r)},
\end{aligned} \tag{22}$$

$$\begin{aligned}
&\mathbb{E}(\nu_V)\\
&= (P+r-1)d+\tau_{\text{enc}}+r\tau_{\text{extra}}\\
&\quad -(d+\tau_{\text{extra}})\frac{\sum_{i=1}^{r-1}P_s(\nu_i)}{P_s(\nu_r)} - \tau_{\text{fb}}.
\end{aligned} \tag{23}$$

Then we calculate, (24), as shown at the bottom of the page.

We simplify the complex expressions as follows, (25)–(28), as shown at the top of the next page.

Then we have $\mathbb{E}(\nu_V)=\alpha+\beta-\tau_{\text{fb}}$, $\frac{\mathbb{E}(T^2)}{2\mathbb{E}(T)}=\gamma+\delta$, $\overline{A}=\alpha+\beta+\gamma+\delta-\tau_{\text{fb}}-\frac{1}{2}$. We can derive that

$$\begin{aligned}
&\alpha+\delta\\
&= \frac{(Pd+r-1+\tau_{\text{enc}}+r\tau_{\text{extra}})^2}{2(Pd+r-1+\tau_{\text{enc}}+r\tau_{\text{extra}}-\sum_{i=1}^{r-1}(1+\tau_{\text{extra}})P_s(\nu_i))}\\
&\quad -\frac{\sum_{i=1}^{r-1}(1+\tau_{\text{extra}})(2Pd+2i-1+2\tau_{\text{enc}}+\tau_{\text{extra}}(2i+1))P_s(\nu_i)}{2(Pd+r-1+\tau_{\text{enc}}+r\tau_{\text{extra}}-\sum_{i=1}^{r-1}(1+\tau_{\text{extra}})P_s(\nu_i))},
\end{aligned} \tag{29}$$

where (29) can be calculated by the complete square, and

$$\begin{aligned}
&\beta+\gamma\\
&= \frac{Pd+r-1+\tau_{\text{enc}}+r\tau_{\text{extra}}-\sum_{i=1}^{r-1}(1+\tau_{\text{extra}})P_s(\nu_i)}{P_s(\nu_r)}.
\end{aligned} \tag{30}$$

$$\begin{aligned}
\frac{\mathbb{E}(T^2)}{2\mathbb{E}(T)} &= -\frac{1}{2}\frac{[(P+r-1)d+\tau_{\text{enc}}+r\tau_{\text{extra}}]^2}{(P+r-1)d+\tau_{\text{enc}}+r\tau_{\text{extra}}-(d+\tau_{\text{extra}})\sum_{i=1}^{r-1}P_s(\nu_i)}\\
&\quad +\frac{1}{2}\frac{\sum_{i=1}^{r-1}(d+\tau_{\text{extra}})^2P_s(\nu_i)(2r-2i-1)}{(P+r-1)d+\tau_{\text{enc}}+r\tau_{\text{extra}}-(d+\tau_{\text{extra}})\sum_{i=1}^{r-1}P_s(\nu_i)}\\
&\quad -\frac{\sum_{i=1}^{r-1}(d+\tau_{\text{extra}})P_s(\nu_i)[(P+r-1)d+\tau_{\text{enc}}+r\tau_{\text{extra}}]}{P_s(\nu_r)(P+r-1)d+\tau_{\text{enc}}+r\tau_{\text{extra}}-(d+\tau_{\text{extra}})\sum_{i=1}^{r-1}P_s(\nu_i)}\\
&\quad +\frac{[(P+r-1)d+\tau_{\text{enc}}+r\tau_{\text{extra}}]^2}{P_s(\nu_r)[(P+r-1)d+\tau_{\text{enc}}+r\tau_{\text{extra}}-(d+\tau_{\text{extra}})\sum_{i=1}^{r-1}P_s(\nu_i)]}.
\end{aligned} \tag{24}$$

$$\alpha = (P+r-1)d + \tau_{\text{enc}} + r\tau_{\text{extra}}, \tag{25}$$

$$\beta = -(d+\tau_{\text{extra}})\frac{\sum_{i=1}^{r-1} P_s(\nu_i)}{P_s(\nu_r)}, \tag{26}$$

$$\gamma = \frac{[(P+r-1)d + \tau_{\text{enc}} + r\tau_{\text{extra}}]^2}{P_s(\nu_r)[(P+r-1)d + \tau_{\text{enc}} + r\tau_{\text{extra}} - (d+\tau_{\text{extra}})\sum_{i=1}^{r-1} P_s(\nu_i)]} - \frac{\sum_{i=1}^{r-1}(d+\tau_{\text{extra}})P_s(\nu_i)[(P+r-1)d + \tau_{\text{enc}} + r\tau_{\text{extra}}]}{P_s(\nu_r)(P+r-1)d + \tau_{\text{enc}} + r\tau_{\text{extra}} - (d+\tau_{\text{extra}})\sum_{i=1}^{r-1} P_s(\nu_i)}, \tag{27}$$

$$\delta = -\frac{1}{2}\frac{[(P+r-1)d + \tau_{\text{enc}} + r\tau_{\text{extra}}]^2}{(P+r-1)d + \tau_{\text{enc}} + r\tau_{\text{extra}} - (d+\tau_{\text{extra}})\sum_{i=1}^{r-1} P_s(\nu_i)} + \frac{1}{2}\frac{\sum_{i=1}^{r-1}(d+\tau_{\text{extra}})^2 P_s(\nu_i)(2r-2i-1)}{(P+r-1)d + \tau_{\text{enc}} + r\tau_{\text{extra}} - (d+\tau_{\text{extra}})\sum_{i=1}^{r-1} P_s(\nu_i)}. \tag{28}$$

By substituting (29) and (30) into $\overline{A} = \alpha+\beta+\gamma+\delta-\tau_{\text{fb}}-\frac{1}{2}$ we can derive the average AoI expression of the HARQ-based Spinal coded system in (13).

REFERENCES

[1] H. Peng, L. Liang, X. Shen, and G. Y. Li, "Vehicular communications: A network layer perspective," *IEEE Trans. Veh. Technol.*, vol. 68, no. 2, pp. 1064–1078, Feb. 2019.

[2] H. Li, Y. Fan, G. Pan, and C. Song, "Event-triggered remote dynamic control for network control systems," in *Proc. 16th Int. Conf. Control, Autom., Robot. Vis. (ICARCV)*, Dec. 2020, pp. 483–488.

[3] S. Kaul, M. Gruteser, V. Rai, and J. Kenney, "Minimizing age of information in vehicular networks," in *Proc. 8th Annu. IEEE Commun. Soc. Conf. Sensor, Mesh Ad Hoc Commun. Netw.*, Jun. 2011, pp. 350–358.

[4] R. D. Yates, "Status updates through networks of parallel servers," in *Proc. IEEE Int. Symp. Inf. Theory (ISIT)*, Jun. 2018, pp. 2281–2285.

[5] A. M. Bedewy, Y. Sun, and N. B. Shroff, "Optimizing data freshness, throughput, and delay in multi-server information-update systems," in *Proc. IEEE Int. Symp. Inf. Theory (ISIT)*, Jul. 2016, pp. 2569–2573.

[6] R. Talak, S. Karaman, and E. Modiano, "Optimizing information freshness in wireless networks under general interference constraints," *IEEE/ACM Trans. Netw.*, vol. 28, no. 1, pp. 15–28, Feb. 2019.

[7] I. Kadota, E. Uysal-Biyikoglu, R. Singh, and E. Modiano, "Minimizing the age of information in broadcast wireless networks," in *Proc. 54th Annu. Allerton Conf. Commun., Control, Comput. (Allerton)*, Sep. 2016, pp. 844–851.

[8] S. Leng and A. Yener, "Age of information minimization for wireless ad hoc networks: A deep reinforcement learning approach," in *Proc. IEEE Global Commun. Conf. (GLOBECOM)*, Dec. 2019, pp. 1–6.

[9] G. D. Nguyen, S. Kompella, C. Kam, J. E. Wieselthier, and A. Ephremides, "Information freshness over an interference channel: A game theoretic view," in *Proc. IEEE INFOCOM Conf. Comput. Commun.*, Apr. 2018, pp. 908–916.

[10] E. T. Ceran, D. Gunduz, and A. Gyorgy, "Average age of information with hybrid ARQ under a resource constraint," *IEEE Trans. Wireless Commun.*, vol. 18, no. 3, pp. 1900–1913, Mar. 2019.

[11] R. D. Yates, E. Najm, E. Soljanin, and J. Zhong, "Timely updates over an erasure channel," in *Proc. IEEE Int. Symp. Inf. Theory (ISIT)*, Jun. 2017, pp. 316–320.

[12] H. Sac, T. Bacinoglu, E. Uysal-Biyikoglu, and G. Durisi, "Age-optimal channel coding blocklength for an M/G/1 queue with HARQ," in *Proc. IEEE 19th Int. Workshop Signal Process. Adv. Wireless Commun. (SPAWC)*, Jun. 2018, pp. 1–5.

[13] A. Arafa, K. Banawan, K. G. Seddik, and H. V. Poor, "On timely channel coding with hybrid ARQ," in *Proc. IEEE Global Commun. Conf. (GLOBECOM)*, Dec. 2019, pp. 1–6.

[14] S. C. Bobbili, P. Parag, and J.-F. Chamberland, "Real-time status updates with perfect feedback over erasure channels," *IEEE Trans. Commun.*, vol. 68, no. 9, pp. 5363–5374, Sep. 2020.

[15] M. Xie, Q. Wang, J. Gong, and X. Ma, "Age and energy analysis for LDPC coded status update with and without ARQ," *IEEE Internet Things J.*, vol. 7, no. 10, pp. 10388–10400, Oct. 2020.

[16] J. You, S. Wu, Y. Deng, J. Jiao, and Q. Zhang, "An age optimized hybrid ARQ scheme for polar codes via Gaussian approximation," *IEEE Wireless Commun. Lett.*, vol. 10, no. 10, pp. 2235–2239, Oct. 2021.

[17] J. Perry, P. A. Iannucci, K. E. Fleming, H. Balakrishnan, and D. Shah, "Spinal codes," in *Proc. ACM SIGCOMM Comput. Commun. Rev.*, Aug. 2012, vol. 42, no. 4, pp. 49–60.

[18] H. Balakrishnan, P. Iannucci, J. Perry, and D. Shah, "De-randomizing Shannon: The design and analysis of a capacity-achieving rateless code," 2012, *arXiv:1206.0418*.

[19] Y. Li, J. Wu, B. Tan, M. Wang, and W. Zhang, "Compressive spinal codes," *IEEE Trans. Veh. Technol.*, vol. 68, no. 12, pp. 11944–11954, Dec. 2019.

[20] X. Yu, Y. Li, W. Yang, and Y. Sun, "Design and analysis of unequal error protection rateless spinal codes," *IEEE Trans. Commun.*, vol. 64, no. 11, pp. 4461–4473, Nov. 2016.

[21] H. Liang, A. Liu, F. Cheng, and X. Liang, "Rateless polar-spinal coding scheme with enhanced information unequal error protection," *IEEE Access*, vol. 7, pp. 145996–146004, 2019.

[22] Y. Hu, R. Liu, H. Bian, and D. Lyu, "Design and analysis of a low-complexity decoding algorithm for spinal codes," *IEEE Trans. Veh. Technol.*, vol. 68, no. 5, pp. 4667–4679, May 2019.

[23] W. Yang, Y. Li, X. Yu, and Y. Sun, "Two-way spinal codes," in *Proc. IEEE Int. Symp. Inf. Theory (ISIT)*, Jul. 2016, pp. 1919–1923.

[24] A. Li, S. Wu, J. Jiao, N. Zhang, and Q. Zhang, "Spinal codes over fading channel: Error probability analysis and encoding structure improvement," *IEEE Trans. Wireless Commun.*, vol. 20, no. 12, pp. 8288–8300, Dec. 2021.

Siqi Meng received the B.E. degree in electronic and information engineering from the Harbin Institute of Technology (Shenzhen) in 2021, where he is currently pursuing the Ph.D. degree with the Department of Electronic Engineering. His research interests include wireless communications and advanced channel coding techniques.

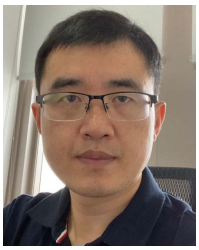

Shaohua Wu (Member, IEEE) received the Ph.D. degree in communication engineering from the Harbin Institute of Technology in 2009. From 2009 to 2011, he held a post-doctoral position at the Department of Electronics and Information Engineering, Shenzhen Graduate School, Harbin Institute of Technology, where he has been since 2012. From 2014 to 2015, he was a Visiting Researcher with the BBCR, University of Waterloo, Canada. He is currently a Full Professor with the Harbin Institute of Technology (Shenzhen), China. He is also a Professor with the Peng Cheng Laboratory, Shenzhen, China. His research interests include satellite and space communications, advanced channel coding techniques, space-air-ground-sea integrated networks, and B5G/6G wireless transmission technologies. He has authored or coauthored over 100 articles in these fields and holds over 40 Chinese patents.

Aimin Li (Student Member, IEEE) received the B.E. degree in electronic and information engineering from the Harbin Institute of Technology (Shenzhen) in 2020, where he is currently pursuing the Ph.D. degree with the Department of Electronic Engineering. His research interests include aerospace communications, advanced channel coding techniques, and wireless communications.

Jian Jiao (Member, IEEE) received the M.S. and Ph.D. degrees in communication engineering from the Harbin Institute of Technology (HIT), Harbin, China, in 2007 and 2011, respectively. From 2011 to 2015, he was a Post-Doctoral Research Fellow with the Communication Engineering Research Centre, Shenzhen Graduate School, HIT, Shenzhen, China. Since 2015, he has been with the School of Electrical and Information Engineering, HIT, where he is currently an Associate Professor. From 2016 to 2017, he was a China Scholarship Council Visiting Scholar with the School of Electrical and Information Engineering, The University of Sydney, Sydney, NSW, Australia. He is also an Associate Professor with the Peng Cheng Laboratory, Shenzhen. His research interests include error control codes, satellite communications, and massive RA.

Ning Zhang (Senior Member, IEEE) received the B.S. degree from Beijing Jiaotong University, China, in 2007, the M.S. degree from the Beijing University of Posts and Telecommunications in 2010, and the Ph.D. degree from the University of Waterloo, Canada, in 2015. After that, he was a Post-Doctoral Research Fellow at the University of Waterloo and the University of Toronto, Canada, respectively. He is currently an Associate Professor with the University of Windsor, Canada. His research interests include connected vehicles, mobile edge computing, wireless networking, and machine learning. He was a recipient of the Best Paper Awards from the IEEE GLOBECOM in 2014, the IEEE WCSP in 2015, the *Journal of Communications and Information Networks* in 2018, the IEEE ICC in 2019, the IEEE Technical Committee on Transmission Access and Optical Systems in 2019, and the IEEE ICCC in 2019. He was the Workshop Chair for MobiEdge 2018 (in conjunction with IEEE WiMob 2018), CoopEdge 2018 (in conjunction with IEEE EDGE 2018), and 5G&NTN 2019 (in conjunction with IEEE EDGE 2019). He serves as an Associate Editor for IEEE INTERNET OF THINGS JOURNAL, IEEE TRANSACTIONS ON COGNITIVE COMMUNICATIONS AND NETWORKING, IEEE ACCESS, and *IET Communications*, and an Area Editor for *Encyclopedia of Wireless Networks* (Springer) and Cambridge Scholars. He also serves/served as a Guest Editor for several international journals, such as IEEE WIRELESS COMMUNICATIONS, IEEE TRANSACTIONS ON COGNITIVE COMMUNICATIONS AND NETWORKING, IEEE ACCESS, and *IET Communications*.

Qinyu Zhang (Senior Member, IEEE) received the bachelor's degree in communication engineering from the Harbin Institute of Technology (HIT), Harbin, China, in 1994, and the Ph.D. degree in biomedical and electrical engineering from the University of Tokushima, Tokushima, Japan, in 2003. From 1999 to 2003, he was an Assistant Professor with the University of Tokushima. From 2003 to 2005, he was an Associate Professor with the Shenzhen Graduate School, HIT, and was the Founding Director of the Communication Engineering Research Center, School of Electronic and Information Engineering (EIE). Since 2005, he has been a Full Professor and the Dean of the EIE School, HIT. He is currently a Professor with the Peng Cheng Laboratory, Shenzhen, China. His research interests include aerospace communications and networks, wireless communications and networks, cognitive radios, signal processing, and biomedical engineering. He has been a TPC Member of the Infocom, IEEE ICC, IEEE GLOBECOM, IEEE Wireless Communications and Networking Conference, and other flagship conferences in communications. He was an Associate Chair for Finance of the International Conference on Materials and Manufacturing Technologies 2012, the TPC Co-Chair of the IEEE/CIC ICCC 2015, and the Symposium Co-Chair of the CHINACOM 2011 and the IEEE Vehicular Technology Conference 2016 (Spring). He was the Founding Chair of the IEEE Communications Society Shenzhen Chapter. He is on the Editorial Board of some academic journals, such as *Journal of Communication*, *KSII Transactions on Internet and Information Systems*, and *Science China Information Sciences*.